Electronic Supplementary Material (ESI) for Materials Chemistry Frontiers.

Supporting Information

Universal Phase Transformation of Ni-Se Electrocatalysts Induced by Electrochemical Activation Strategy for Significantly Enhanced Alkaline Hydrogen Evolution Reaction

Li-Wen Jiang[a], Zhao-Hua Yin[a], Hong Liu[a,c,*], and Jian-Jun Wang[a,b,*]

[a] State Key Laboratory of Crystal Materials, Shandong University, Jinan, Shandong 250100, China

[b] Shenzhen Research Institute of Shandong University, Shenzhen, 518057, China

[c] Institute for Advanced Interdisciplinary Research (IAIR), University of Jinan, Jinan 250022, China

Experimental section

Chemicals:

$Ni(NO_3)_2·6H_2O$, $NaBH_4$, and KOH were bought from Sinopharm Chemical Reagent Co., Ltd, Shanghai, China and Se powder was obtained from Aladdin Ltd., Shanghai, China. All the chemicals were directly used as received without further purification.

Electrodeposition of $Ni(OH)_2$ on carbon cloth:

Typically, a piece of carbon cloth (CC) was first treated with oxygen plasma to improve its hydrophilicity, and then cleaned by sonication sequentially in acetone, water and ethanol for 10 min, respectively. The electrodeposition of $Ni(OH)_2$ was carried out using a standard three-electrode system on an electrochemistry workstation (CHI 660E). A Pt foil and Ag/AgCl (3 M KCl) were used as the counter electrode and the reference electrode, respectively, and a piece of carbon cloth (2×2 cm) was used as the working electrode. An aqueous solution of 0.1 M $Ni(NO_3)_2$ was prepared as the electrolyte. The electrodeposition was conducted at a constant potential of −1 V vs Ag/AgCl for 20 min. After deposition, the as-prepared $Ni(OH)_2$ electrode was washed with water for several times and dried at 60℃ in vacuum.

Synthesis of $Ni_{0.85}Se$ on carbon cloth:

In a typical experiment, 59 mg of Se power and 65 mg of $NaBH_4$ were dissolved into 30 mL of water and the resultant mixture was stirred until a transparent solution was obtained. Then, the prepared solution with a piece of the fabricated $Ni(OH)_2$ electrode was transferred into a Teflon-lined stainless-steel autoclave (50 mL) and the autoclave was sealed and maintained at 180℃ for 24 h in an oven. After cooling naturally down

to room temperature, the sample was washed with water for several times and then dried at 60℃ in vacuum.

Characterizations:

The structures and morphologies of the samples were studied by scanning electron microscopy (SEM) on a Hitachi S-4800 field emission scanning electron microscopy and transmission electron microscopy (TEM) with energy dispersive X-ray spectroscopy (EDX) on JEOL JEM-2100 at 200 kV and Oxford X-Max. Powder X-ray diffraction (XRD) patterns were obtained by Bruker D8 ADVANCE with a Cu Kα radiation sourcce (λ = 0.154178 nm). X-ray photoelectron spectroscopy (XPS) analysis was performed on a Thermo Fisher ESCALAB XI+. Raman spectra was recorded on microscopic Raman spectrometer (HORIBA Lab RAM HR Evolution) with a laser of 532 nm. Electron paramagnetic resonance (EPR) spectra were collected on a Bruker A300 spectrometer at the frequency of 9.853GHz at 298 K. The inductively coupled plasma mass spectrometer (ICP-MS) results were acquired by PerkinElmer NexION 350X.

Electrochemical measurements:

The electrochemical measurements were performed using a standard three-electrode system with 1 M KOH as the electrolyte on the CHI 660E electrochemical station (CH Instruments, Inc., Shanghai), consisting of the prepared samples on carbon cloth as the working electrode, Hg/HgO (1 M KOH) as the reference electrode, and a graphite rod as the counter electrode. The electrochemical activation was carried out by repetitive scans of Linear Sweep Voltammetry (LSV) between -0.8 V and -1.6 V

(vs Hg/HgO) at a scan rate of 5 $mV \cdot s^{-1}$. For all the experiments, the working surface area of the electrode was controlled to 1×0.5 cm and tests were carried out at ambient temperature. All the measured potentials were converted to a reversible hydrogen electrode (RHE) according to the equation: $E_{(RHE)}=E_{(Hg/HgO)}+0.059\times pH+0.098$ V. To obtain the electrochemical double layer capacitance (C_{dl}), the cyclic voltammetry (CV) was swept between 0.024 V and 0.124 V (vs RHE) at varied scan rates (20, 40, 60, 80, 100, and 120 mV s^{-1}) because no apparent faradaic reactions were observed in this potential range for all the electrodes. The electrochemical impedance spectroscopy (EIS) was measured at -0.1 V (vs RHE) from 100 kHz to 0.01 Hz with an AC amplitude of 5 mV. For long-term stability tests, the chronopotentiometry (CP) curves were recorded at a current density of -20 mA cm^{-2} and the chronoamperometric (CA) curves were obtained at an overpotential of 176 mV. All the measured potentials were not calibrated with iR compensation.

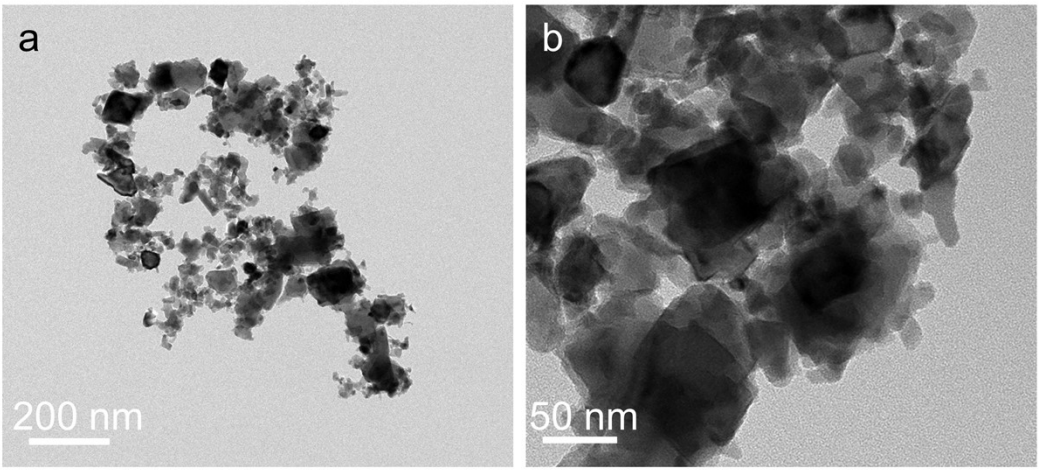

Figure S1. TEM images at different magnifications for $Ni_{0.85}Se$.

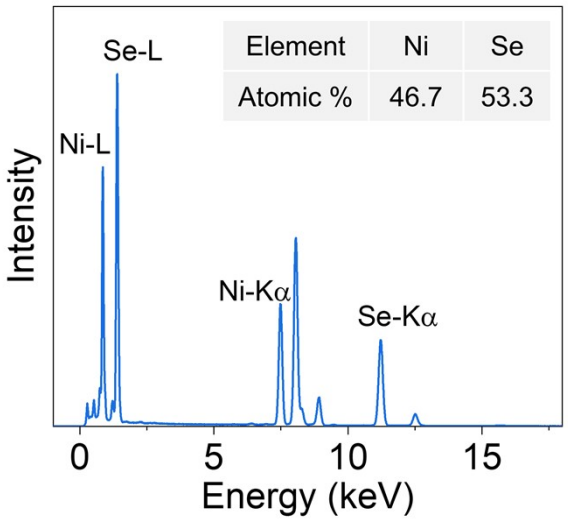

Figure S2. EDX spectra and the corresponding atomic ratio of Ni/Se for $Ni_{0.85}Se$.

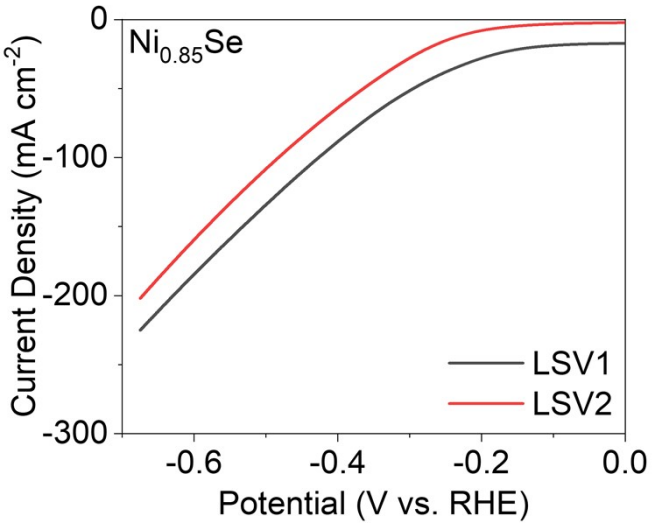

Figure S3. The first and second LSV curves of $Ni_{0.85}Se$.

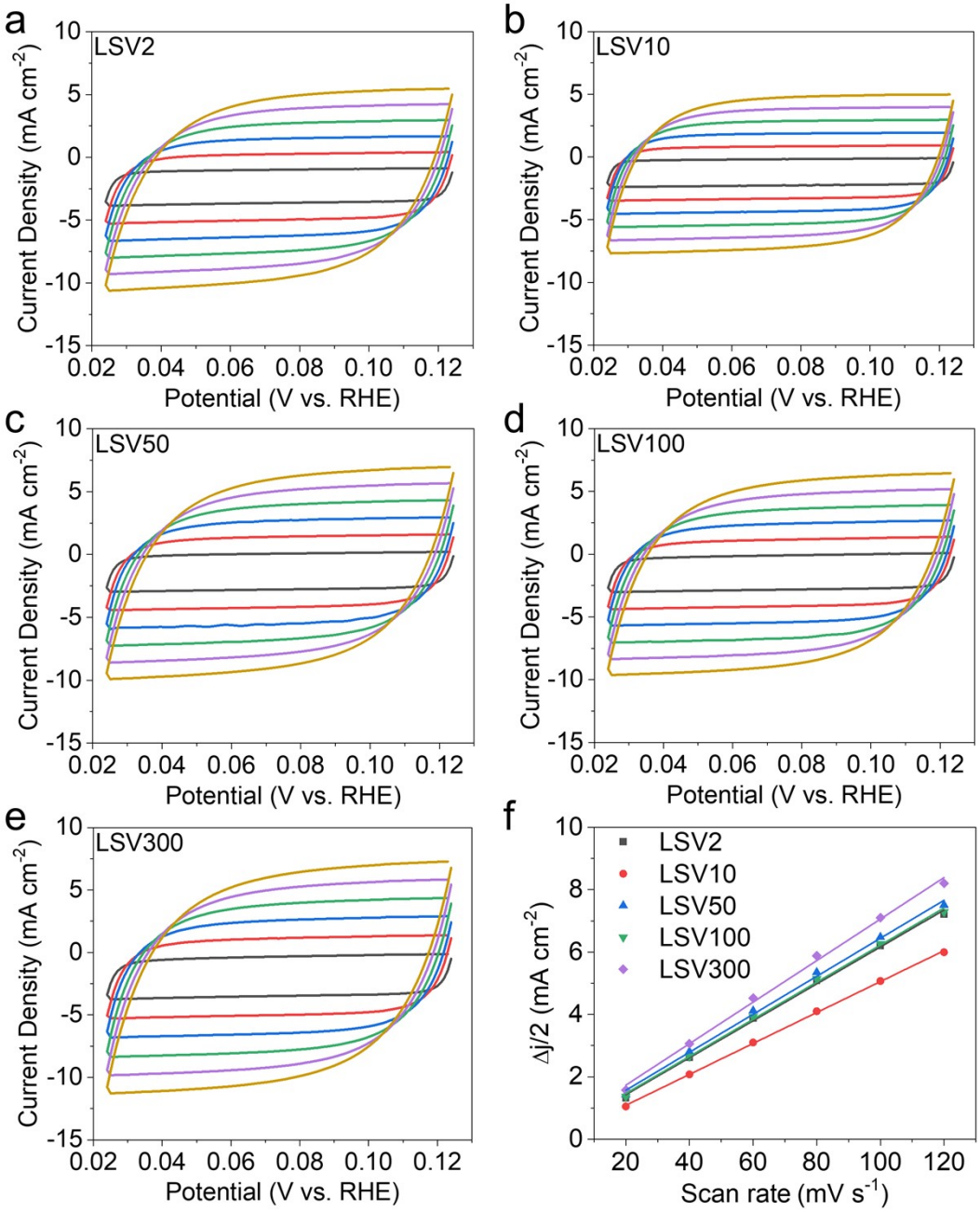

Figure S4. (a-e) CV curves at varied scan rates and (f) the corresponding C_{dl} values of $Ni_{0.85}Se$ after different LSV scans.

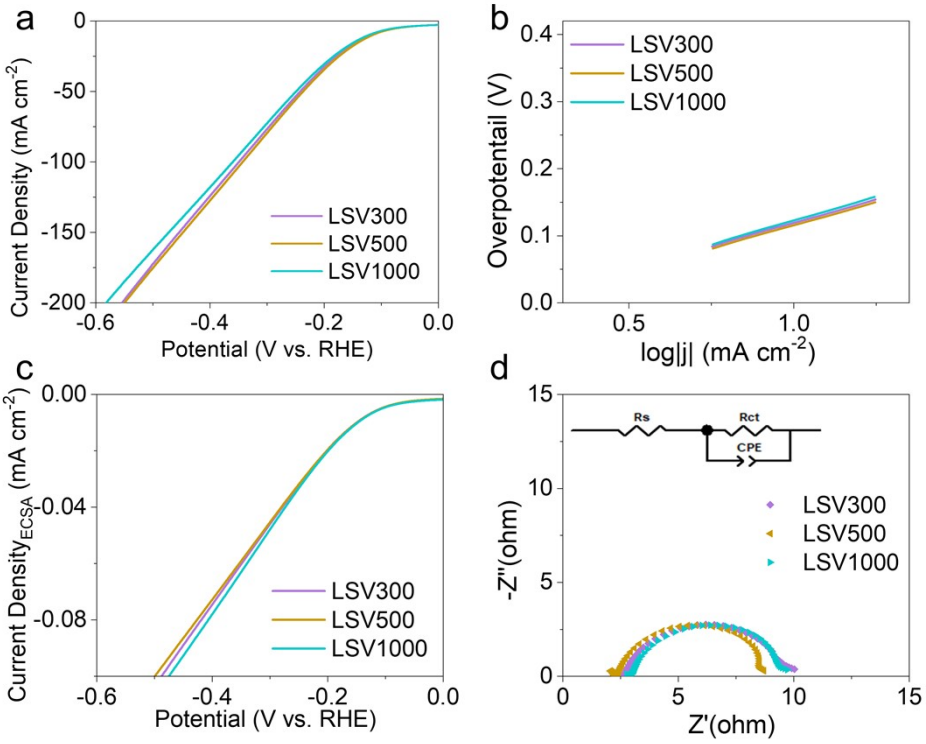

Figure S5. (a) LSV curves, (b) Tafel slopes, (c) ECSA-normalized LSV curves, and (d) Nyquist plots of the $Ni_{0.85}Se$ after different LSV scans in 1 M KOH.

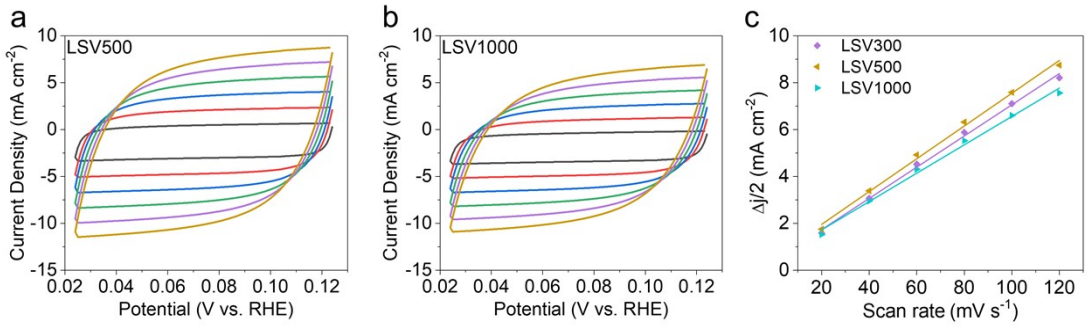

Figure S6. (a, b) CV curves at varied scan rates and (c) the corresponding C_{dl} values of $Ni_{0.85}Se$ after different LSV scans.

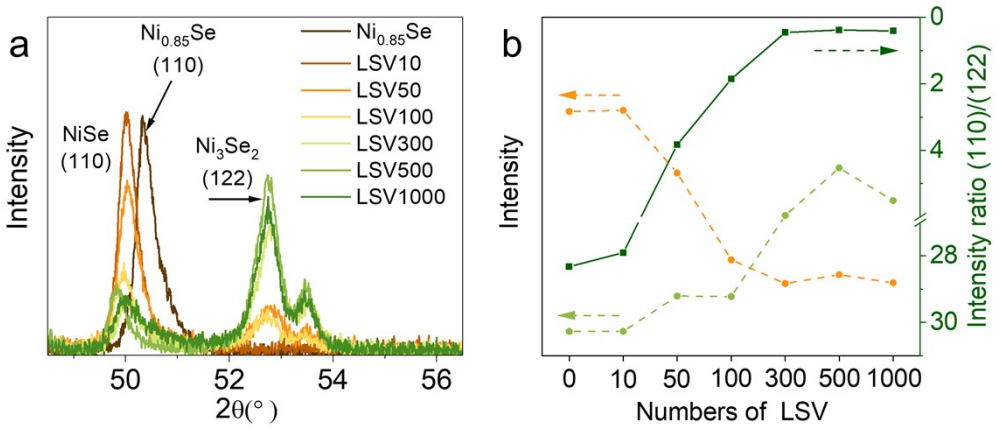

Figure S7. (a) the amplification diffraction patterns, (b) the corresponding intensity ratio of crystal facets during activation process.

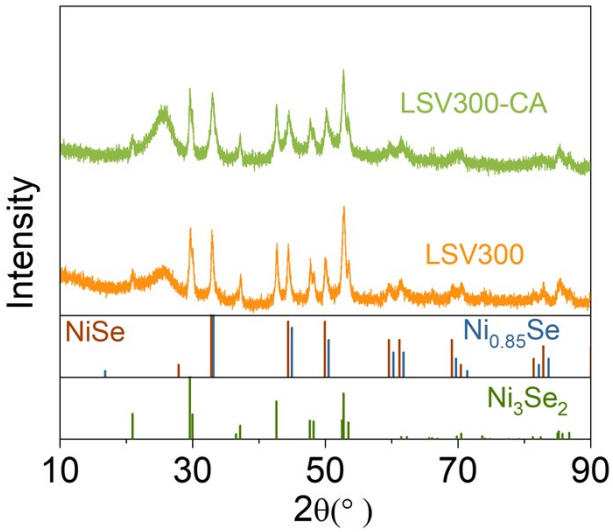

Figure S8. The XRD patterns of the activated $Ni_{0.85}Se$ (after 300 LSV scans) after CA.

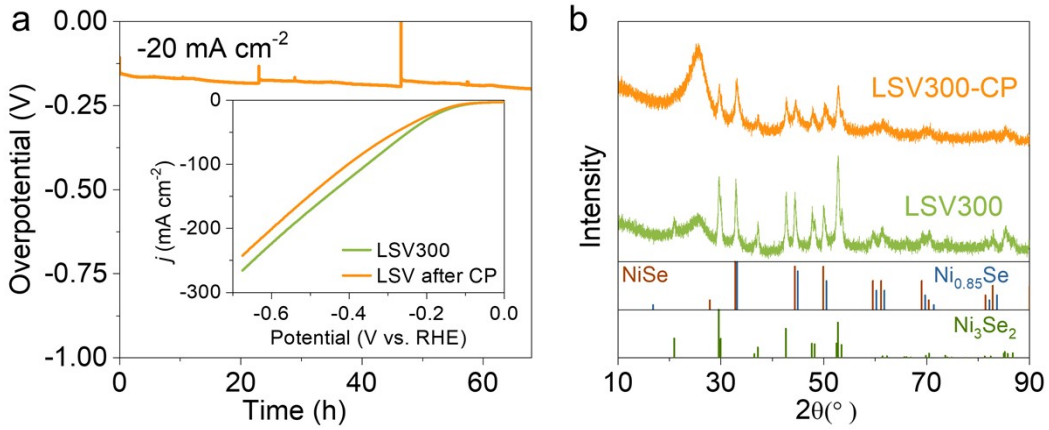

Figure S9. (a) CP curve at a current density of -20 mA cm^{-2} for the activated $Ni_{0.85}Se$ (inset: the LSV curves after CP). (b) The XRD patterns of the activated $Ni_{0.85}Se$ (after 300 LSV scans) after CP.

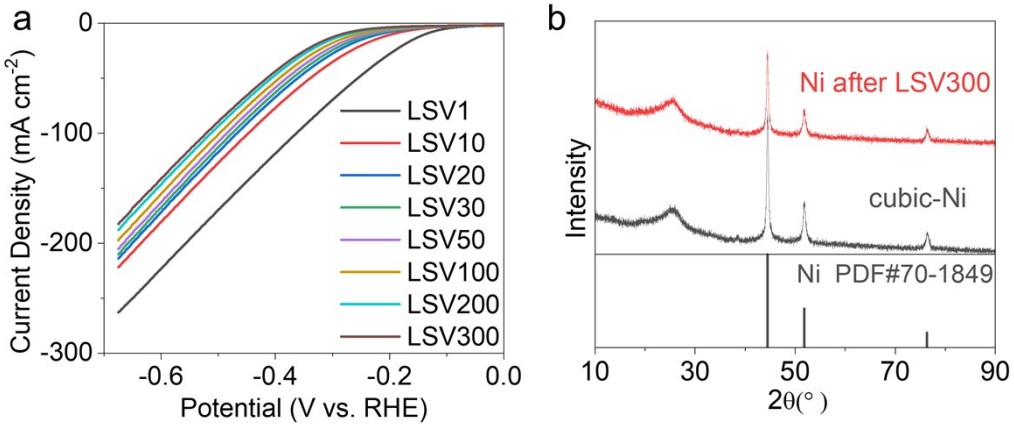

Figure S10. (a) LSV curves and (b) the corresponding XRD patterns of the cubic-Ni before and after 300 LSV scans.

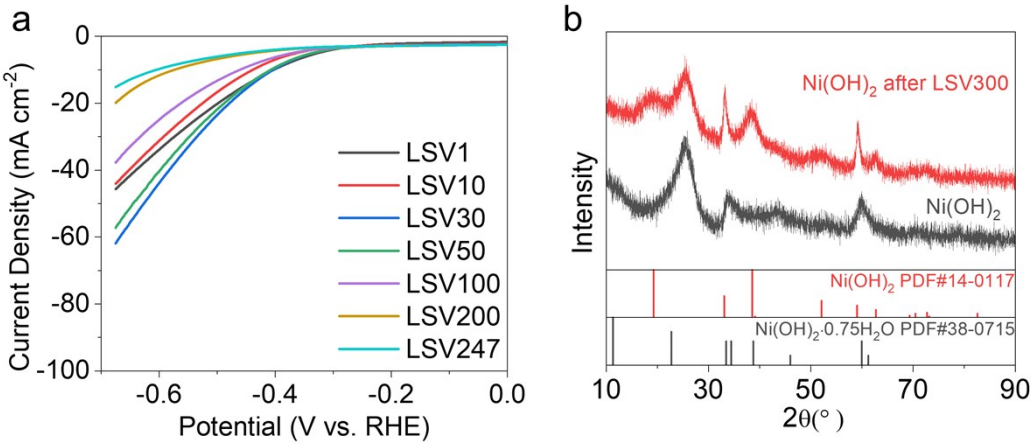

Figure S11. (a) LSV curves and (b) the corresponding XRD patterns of the electrodeposited $Ni(OH)_2$ before and after 300 LSV scans.

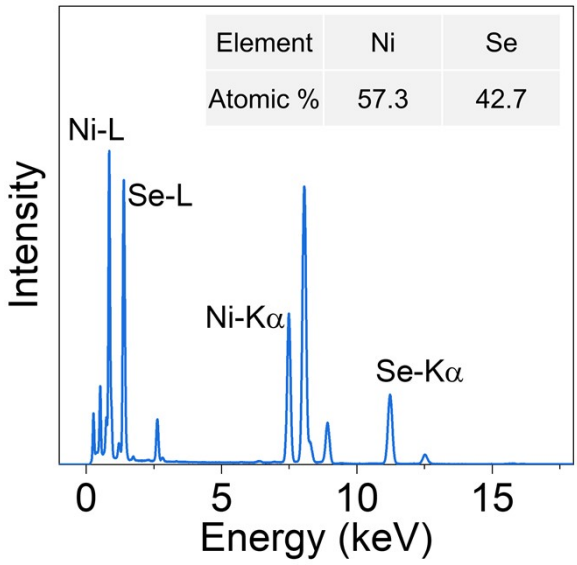

Figure S12. EDX spectra and the corresponding atomic ratio of Ni/Se for $Ni_{0.85}Se$ after 300 LSV scans.

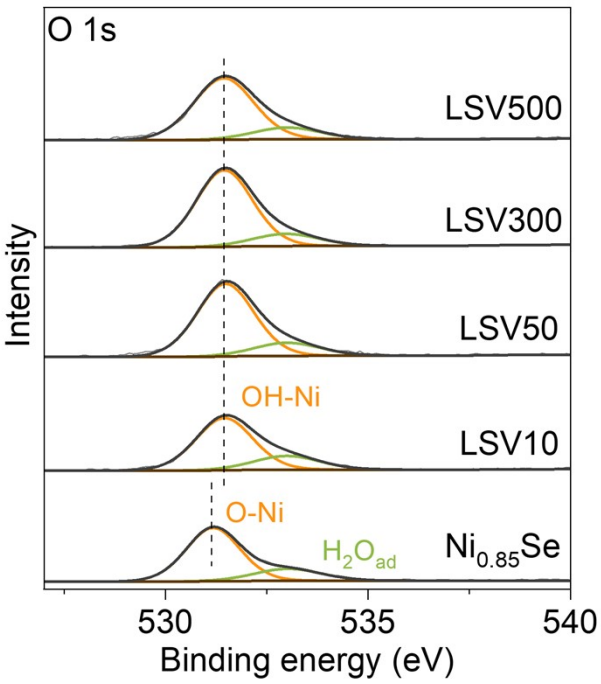

Figure S13. High-resolution XPS spectra of O 1s of the $Ni_{0.85}Se$ at different LSV scans.

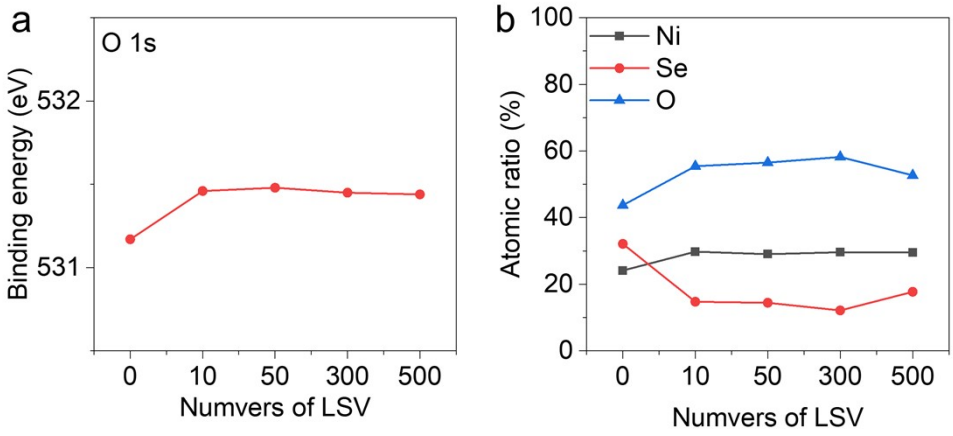

Figure S14. (a) Variation of bonding energy of the fitted O-Ni peak, and (d) comparison of atomic ratio of Ni, Se and O for $Ni_{0.85}Se$ after different LSV scans from XPS.

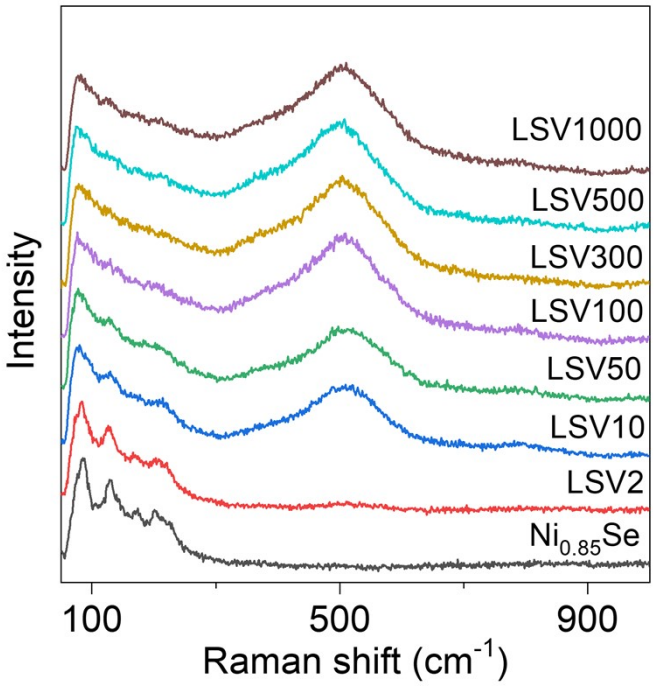

Figure S15. Raman spectrum of the $Ni_{0.85}Se$ at different LSV scans.

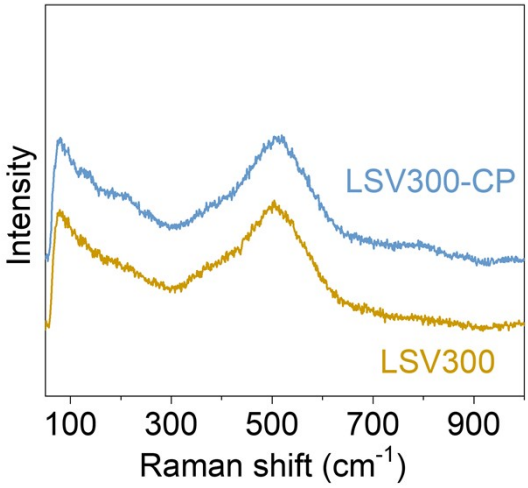

Figure S16. Raman spectra of the activated $Ni_{0.85}Se$ (after 300 LSV scans) after CP.

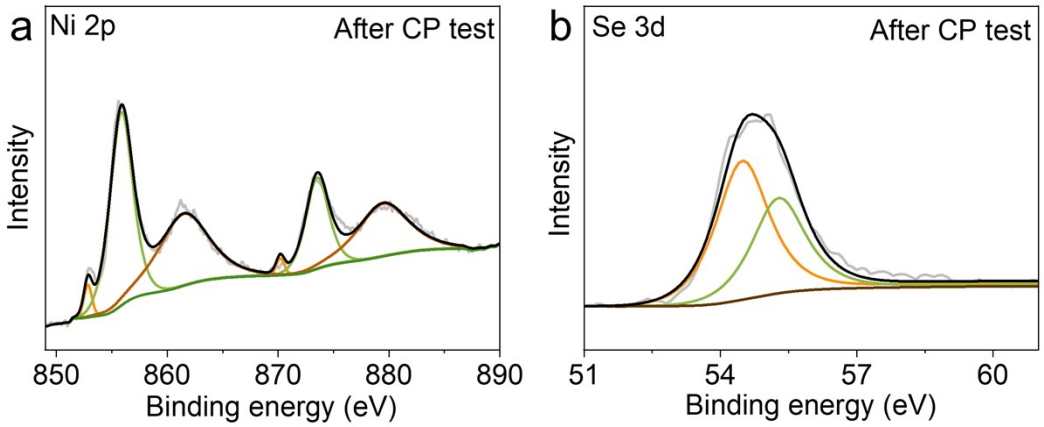

Figure S17. High-resolution XPS spectra of (a) Ni 2p and (b) Se 3d of the activated $Ni_{0.85}Se$ (after 300 LSV scans) after CP.

For Ni 2p, the two peaks at 852.84 and 870.20 eV can be well attributed to Ni $2p_{3/2}$ and Ni $2p_{1/2}$ of Ni-Se. As for Se 3d, the two peaks located at 54.49 and 55.29 eV can be assigned to Se $3d_{5/2}$ and Se $3d_{3/2}$ of Se-Ni.

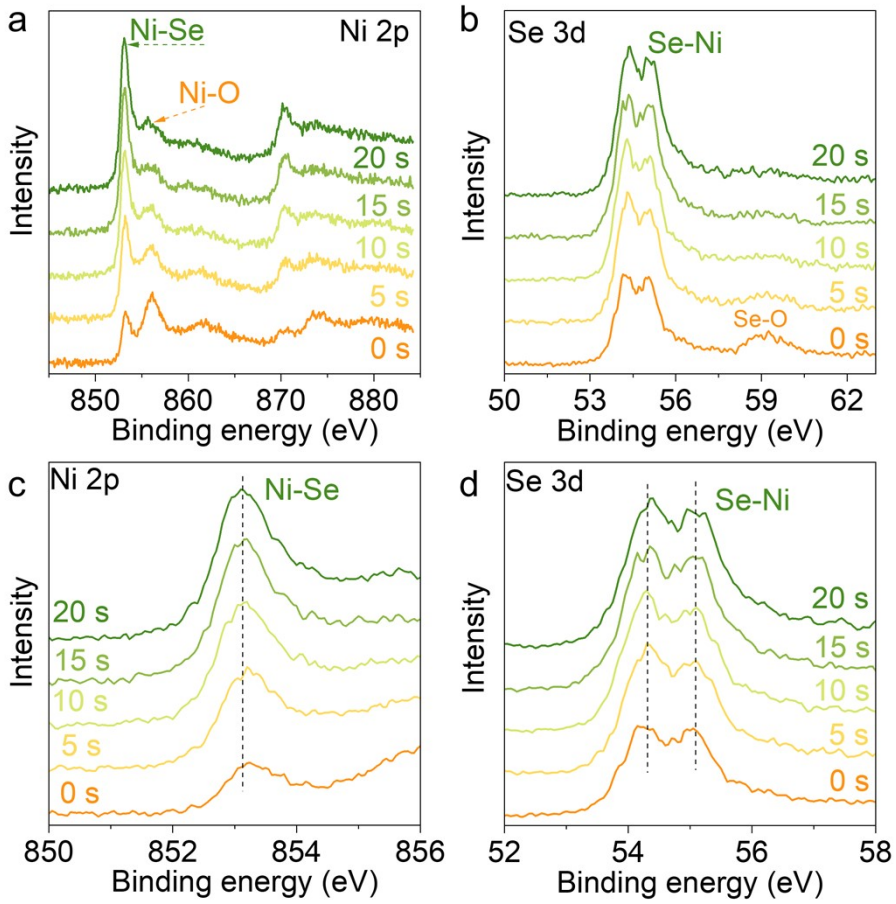

Figure S18. (a, b) XPS spectra and (c, d) enlarged XPS spectra of Ni 2p and Se 3d of the $Ni_{0.85}Se$ etched by Ar ions for different time.

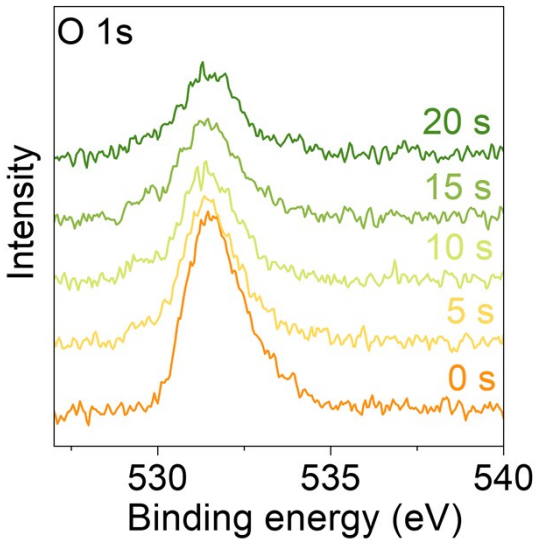

Figure S19. XPS spectra of O 1s of the $Ni_{0.85}Se$ etched by Ar ions for different time.

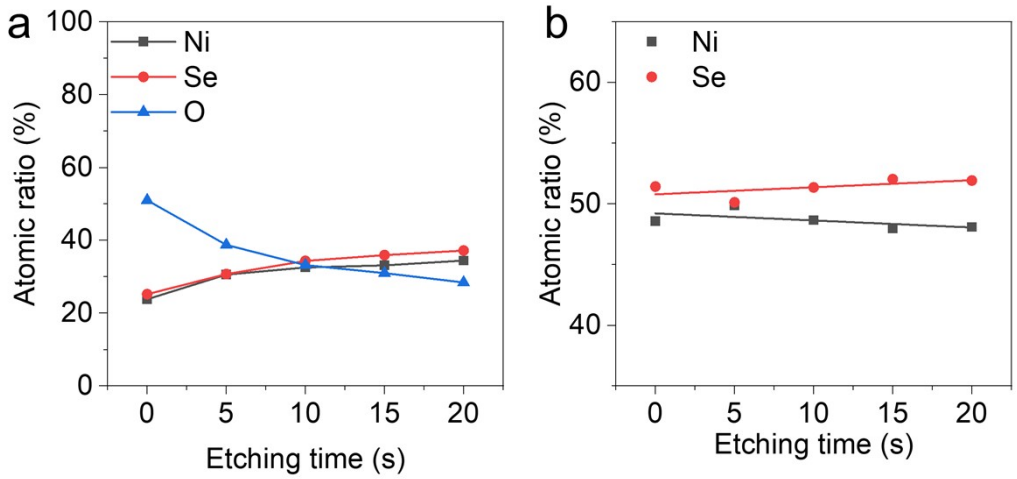

Figure S20. Comparison of atomic ratio of (a) Ni, Se and O, (b) Ni and Se for the $Ni_{0.85}Se$ etched by Ar ions for different time.

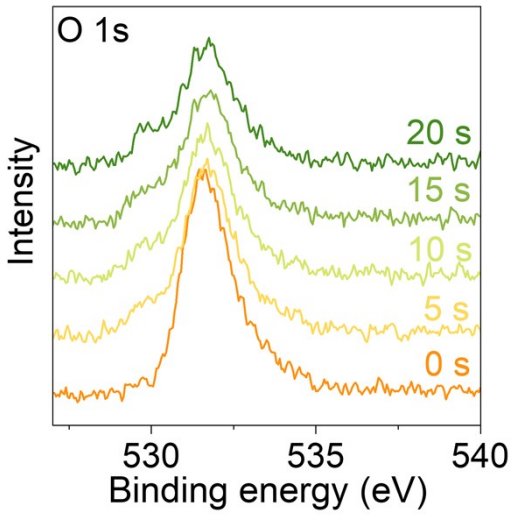

Figure S21. XPS spectra of O 1s of the activated $Ni_{0.85}Se$ (after 300 LSV scans) etched by Ar ions for different time.

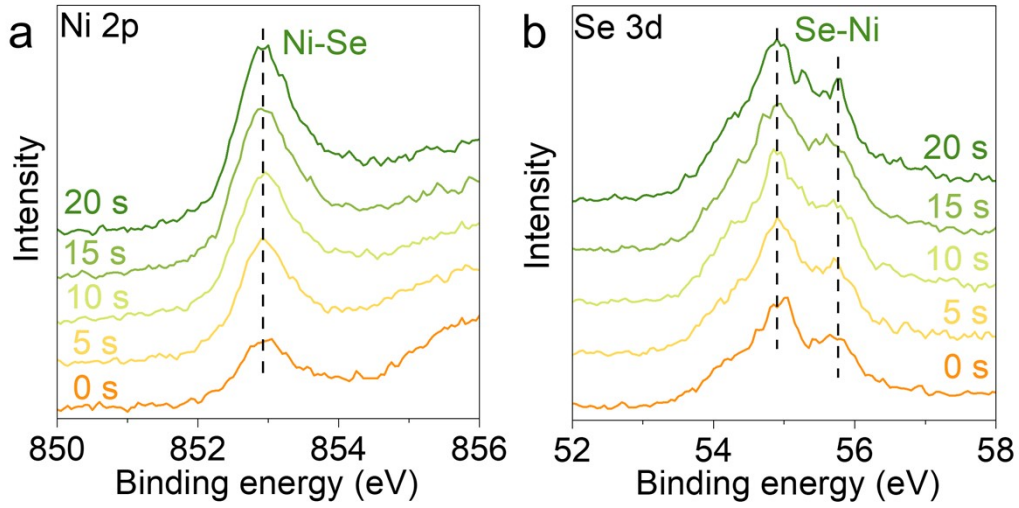

Figure S22. Enlarged XPS spectra of Ni 2p and Se 3d of the activated $Ni_{0.85}Se$ (after 300 LSV scans) etched by Ar ions for different time.

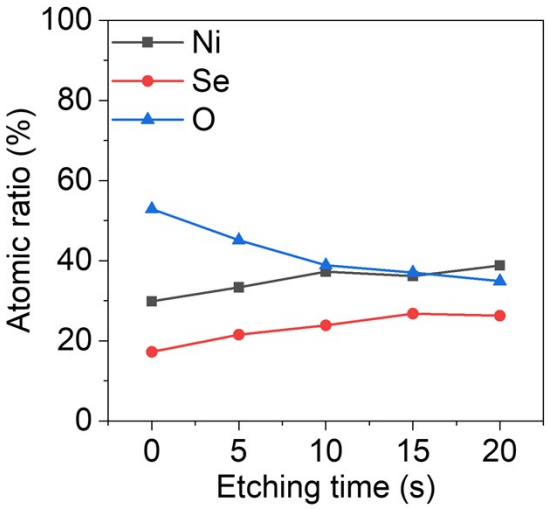

Figure S23. Comparison of atomic ratio of Ni, Se and O for the activated $Ni_{0.85}Se$ (after 300 LSV scans) etched by Ar ions for different time.

Table S1. The fitting Tafel slopes of $Ni_{0.85}Se$ at different LSV scans.

	LSV2	LSV10	LSV50	LSV100	LSV300	LSV500	LSV1000
Tafel ($mV\ dec^{-1}$)	184	226	144	141	138	137	142

Table S2. The calculated C_{dl} values of $Ni_{0.85}Se$ after different LSV scans.

	LSV2	LSV10	LSV50	LSV100	LSV300	LSV500	LSV1000
C_{dl} ($mF\ cm^{-2}$)	59.24	49.62	60.96	59.53	66.62	70.01	60.54

Table S3. The fitted parameters of the EIS data of $Ni_{0.85}Se$ after different LSV scans.

	R_s	R_{ct}	CPE-T	CPE-P
LSV2	2.92	177.5	0.039	0.861
LSV10	2.63	106.8	0.029	0.914
LSV50	2.77	16.0	0.039	0.884
LSV100	2.71	14.6	0.037	0.870
LSV300	2.60	7.1	0.051	0.823
LSV500	2.31	6.8	0.051	0.847
LSV1000	2.91	6.8	0.044	0.844

Table S4. The content of Ni and Se in the electrolyte after different LSV scans.

LSV	10	30	50	100	200	300
Ni (mmol/L)	0.047	0.027	0.044	0.015	0.025	0.006
Se (mmol/L)	0.075	0.091	0.222	0.273	0.318	0.340

Table S5. The fitted bonding energy of Ni 2p and Se 3d and the corresponding atomic ratio of Ni and Se for $Ni_{0.85}Se$ after different LSV scans from XPS.

	Ni 2p (eV)	Se 3d (eV)	Ni	Se
$Ni_{0.85}Se$	853.34	54.32	43%	57%
LSV10	852.92	54.34	67%	33%
LSV50	852.87	54.44	67%	33%
LSV300	852.85	54.51	71%	29%
LSV500	852.83	54.55	63%	37%

Table S6. Variation of bonding energy of the fitted O-Ni peak and the corresponding atomic ratio of Ni, Se and O for $Ni_{0.85}Se$ after different LSV scans from XPS.

	O 1s (eV)	O	Ni	Se
$Ni_{0.85}Se$	531.17	44%	24%	32%
LSV10	531.46	55%	30%	15%
LSV50	531.46	57%	29%	14%
LSV300	531.45	58%	30%	12%
LSV500	531.44	53%	30%	17%

Table S7. Variation of atomic ratio of Ni, Se and O for the $Ni_{0.85}Se$ etched by Ar ions for different time.

Etching time (s)	Ni	Se	O
0	23.8%	25.2%	51.0%
5	30.6%	30.7%	38.7%
10	32.5%	34.3%	33.2%
15	33.1%	35.9%	31.0%
20	34.4%	37.2%	28.4%

Etching time (s)	Ni	Se
0	48.6%	51.4%
5	49.9%	50.1%
10	48.7%	51.3%
15	48.0%	52.0%
20	48.1%	51.9%

Table S8. Variation of atomic ratio of Ni, Se and O for the activated $Ni_{0.85}Se$ (after 300 LSV scans) etched by Ar ions for different time.

Etching time (s)	Ni	Se	O
0	29.9%	17.2%	52.9%
5	33.3%	21.5%	45.2%
10	37.3%	23.9%	38.8%
15	36.2%	26.8%	37.0%
20	38.8%	26.3%	34.9%

Etching time (s)	Ni	Se
0	63.4%	36.6%
5	60.8%	39.2%
10	61.0%	39.0%
15	57.5%	42.5%
20	59.6%	40.4%